Modeling Excitable Systems

Jarrett L. Lancaster* and Edward H. Hellen†

University of North Carolina Greensboro,

Department of Physics and Astronomy, Greensboro, NC 27402

(Dated: July 4, 2008)

Abstract

Excitable media are an important type of nonlinear dynamical system. We present mathematical and electronic models of excitable systems relevant to cardiac and neural systems. These models can serve as building blocks for a variety of investigations of excitable dynamics.

I. INTRODUCTION

Excitable media are an important type of nonlinear system. Excitable systems have a fast-response positive feedback mechanism followed by a slow-response inhibition which causes a recovery phase that returns the system to resting values. The excitation is manifested by the temporal pulse shape of some variable of the system. Important examples in biology are voltages across membranes in cardiac and neural tissue, and calcium waves inside cells. Slower examples are populations during epidemics and vegetation during forest fires. Modeling excitable systems allows exploration of the dynamics of these systems and potentially control of the dynamics for desired outcomes such as cardiac defibrillation, vaccine intervention, and fire-fighting strategies.

Here we present two approaches to investigating excitable systems through mathematical and electronic modeling. One approach is to start with a mathematically simple excitable system and then build its electronic circuit realization. For this approach we use the Fitzhugh-Nagumo (FN) equations.[1,2] The other approach is to start with a simple circuit that exhibits excitable behavior, then find its mathematical model. For this we use a simple 3-transistor excitable circuit. The electronic circuits provide real systems from which measurements may be made and control of behavior attempted. These models provide building blocks from which a variety of experiments may be designed. We demonstrate the examples of a reaction-diffusion excitable medium and pacing stimulation of an excitable system. Recently Yuan et. al. used the FN model for an investigation of spiral waves and chaos in a 2-dimensional excitable medium.[3]

Nagumo constructed a circuit based on the FN equations that uses a tunnel diode for the nonlinear element.[2] Tunnel diodes are no longer inexpensive and readily available, therefore we replace it by analog circuitry. This has the added benefit of being able to easily change the functional form of the nonlinear behavior.

Bunton et. al. describe an excitable circuit based on comparators and multiplexer integrated circuits.[4] They also give a nice review of other circuit models. Part of the appeal of their circuit is its simplicity, the behavior is understood by the action of a four-position switch without the use of equations. In this paper we emphasize finding and using two-variable models in the form of coupled first-order differential equations to predict the behavior of the circuits. Numerical solution of the differential equations is easy to do with today's desk-

top computers using Python, as we did, or any of the popular programming environments. These projects are intended to provide valuable experience with computational physics and circuit analysis and construction.

II. FITZHUGH-NAGUMO MODEL

The Fitzhugh-Nagumo equations are a two-variable simplification of the four-variable Hodgkin-Huxley model for membrane potential in neural tissue.[1,2] The FN system is:

$$\frac{du}{dt} = u\,(u-a)\,(1-u) - v + s\,(t) \tag{1a}$$

$$\frac{dv}{dt} = \epsilon\,(u - bv) \tag{1b}$$

Typical values of parameters that result in excitable behavior are $a = 0.15$, $\epsilon = 0.006$,

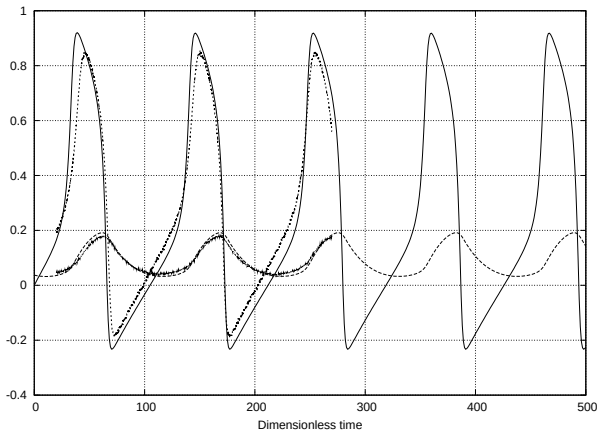

FIG. 1: Numerical computation and experimental data (from about 20 to 280 time units) for excitation pulses for the Fitzhugh-Nagumo system. Voltage and time are dimensionless (see text).

$b = 2.5$. The slow response of variable v is ensured by the small value of ϵ. Function $s\,(t)$ is a source term. For example, setting $s\,(t) = 0.045$ makes Eq 1 autonomous and results in periodic excitation pulses as shown in the plots of u and v in Figure 1. Actual data from a circuit described below is also shown. The threshold nature of the excitation is seen by noting the rapid rise in u as it surpasses the value $a = 0.15$. Alternatively, stimulation pulses can be provided by using a pulse train for $s\,(t)$ in which case Eq 1 is nonautonomous.

Figure 2 shows the phase space trajectory of the excitation pulses shown in Fig. 1 and the nullclines of Eq. 1. The u-nullcline is nonlinear and has the reverse-N shape characteristic of systems that support excitation pulses. Fixed points occur at the intersection of the

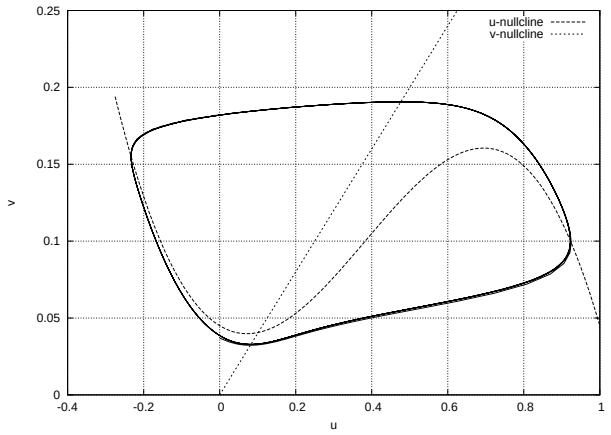

FIG. 2: Numerical computation of phase-space plots of excitation pulses and nullclines for Fitzhugh-Nagumo system with source term $s\,(t) = 0.045$.

nullclines where the time derivatives of u and v are both zero. For the case shown with $s\,(t) = 0.045$ the fixed point is unstable resulting in the cyclic phase space trajectory. For $s\,(t) = 0$ the nullclines intersect at the origin so it is easy to use the Jacobian of Eq 1 in a linearization stability analysis to show that the origin is a stable fixed point characterized as a spiral node.[5]

The circuit we use shown in Fig 3 for the FN system is basically the one used by Nagumo in which the tunnel diode is replaced by a circuit that produces voltage V' which is a cubic function of the capacitor voltage V.[2] The input impedance to the $V'\,(V)$ circuit block is high so that current at its input can be assumed to be zero. Voltage V and inductor current i are the variables analogous to u and v in Eq. 1. The first-order differential equations for

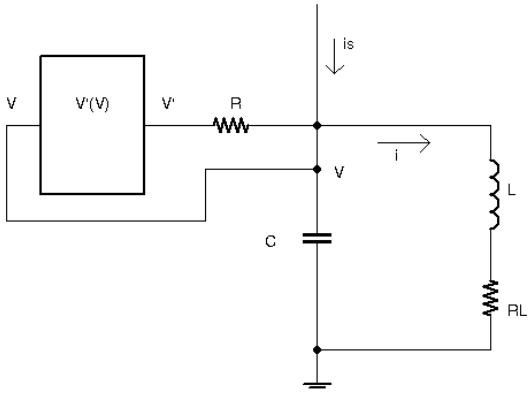

FIG. 3: Schematic for Fitzhugh-Nagumo circuit. $R = 100\Omega, C = 0.1\mu f, L = 0.1H$. R_L accounts for the inductor's intrinsic resistance (220Ω) and an external resistor (33Ω).

V and i are:

$$C\frac{dV}{dt} = \frac{V' - V}{R} - i + i_s \tag{2a}$$

$$\frac{di}{dt} = \frac{1}{L}\left(V - iR_L\right) \tag{2b}$$

These equations are made equivalent to Eq 1 by using dimensionless time $t/(RC)$, $v = iR$, $s\,(t) = i_s R$, and identifying $\epsilon = R^2C/L$ and $b = R_L/R$. The voltage V' is constructed so that $V' - V$ corresponds to the nonlinear term $u(u-a)(1-u)$.

Component values are chosen so that $\epsilon \approx 0.01$ and $b \approx 2.5$. In order to avoid the speed limitations of the op amps and the MLT04 multiplier we choose the time constant RC to be 10 μsec by using $R = 100\Omega$ and $C = 0.10\mu$f. The inductor has intrinsic resistance of 2.2 Ω/mH so an inductor resistance of $R_L = 250\Omega$ corresponding to $b = 2.5$ gives $L = 0.114$ H. However it is convenient to include an external resistance in series with the inductor so that the inductor current may easily be measured from the voltage across the resistor. Using 33Ω leaves about 220Ω for a nominal value $L = 0.10$H. R_L in Fig 3 accounts for both the inductor's resistance and the external 33Ω.

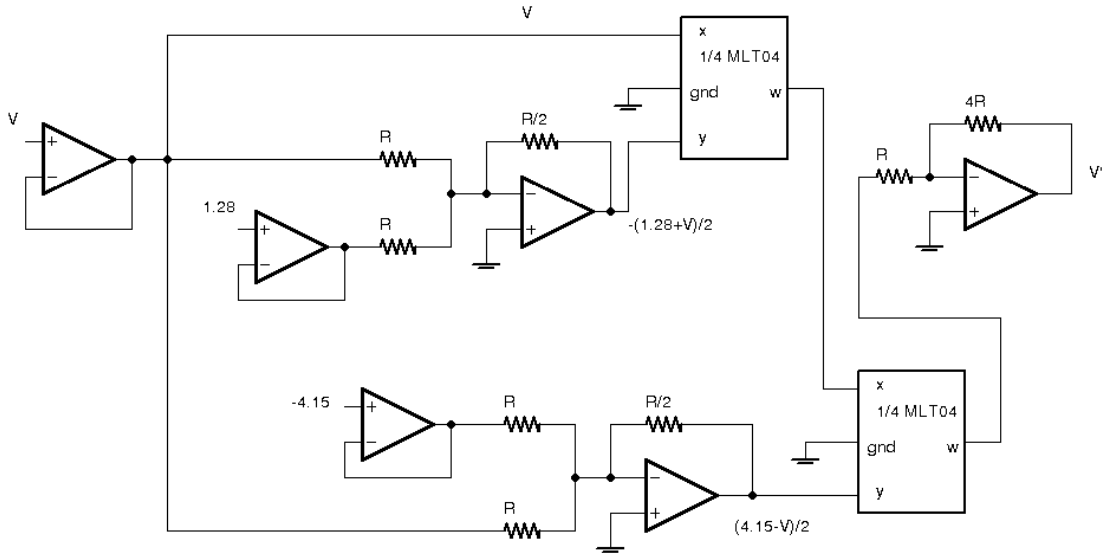

FIG. 4: Circuit for calculation of function $V'\,(V)$. Only 2 of the MLT04's 4 multipliers are used. The unused multipliers (not shown) should be grounded. $R = 6.8k\Omega$.

The voltage V' is a function of V. Both voltages need to be normalized by the scaling factor of the multiplier IC, 2.5 volts for the MLT04. With $u = V/2.5$ the required function

for $u' = V'/2.5$ is

$$u' = u\,(u-a)\,(1-u) + u \tag{3a}$$

$$= -u\,(u-r_1)\,(u-r_2) \tag{3b}$$

For $a = 0.15$ the roots r_1 and r_2 are 1.66 and -0.512. Figure 4 shows the circuit used to create V' from V and the roots of Eq 3. The roots are multiplied by 2.5 giving the values -4.15 and 1.28 volts shown Fig 4. The resulting polynomial factors are divided by 2 by the inverting addition amplifiers prior to the multiplier IC to bring the voltages within the ± 2.5 volt range of the multiplier. Therefore the result after the multipliers is amplified by 4 at the final inverting amplifier. Using potentiometers to set the values -4.15 and 1.28 volts makes it easy to change the roots in Eq 3. Comte and Marquié use a circuit with four fewer op amps to create a cubic polynomial.[6] This reduction in circuit components comes at the expense of not being able to adjust the function so easily. They use their circuit in a simulation of nerve signal propagation using a FN lattice.[7]

We purposely used inexpensive op amps (LF412) and multiplier IC (MLT04) to demonstrate that high precision components are not required in order to obtain results as shown in Fig 1. The prediction uses measured component values which were close to their nominal values. The measured capacitor voltage shown in Fig 1 was normalized by the MLT04's scaling factor of 2.5 volts. The inductor current was obtained from the voltage across the external 33Ω and then multiplied by $R = 100$ to obtain dimensionless v.

A constant source term i_s is provided by the circuit shown in Fig 5. The current i_s is simply the voltage drop across R_E divided by R_E. The emitter voltage is approximately 0.65 volts above the base voltage due to the forward biased emitter-base junction. As an example, $R_1 = 22k\Omega$ and $R_2 = 6.8k\Omega$ gives a base voltage of 3.82 volts. For $R_E = 1k\Omega$ the current is 0.5 ma. This corresponds to $s\,(t) = i_s R = 0.05$ in Eq 1a for $R = 100\Omega$ in Fig 3. Using a $25k\Omega$ potentiometer for R_2 allows for setting $s\,(t)$ in the range 0 to 0.2.

A pulse train for the current source i_s is provided by the circuit in Fig 6 based on a 555 timer. The train's period and each pulse's width and amplitude are controlled by R_a, R_b, and R_E, respectively. For example, with values $R_a = 10k\Omega$, $R_b = 1k\Omega$, and $R_E = 750\Omega$ the period, width, and height are approximately $800\mu s$, $70\mu s$, and $1.2ma$, respectively.

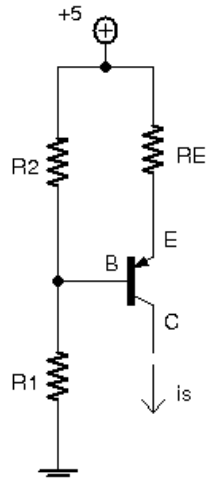

FIG. 5: Constant current source. $R_1 = 22k\Omega$, $R_2 = 6.8k\Omega$, and $R_E = 1k\Omega$ gives $i_s = 0.5$ma. Transistor is general purpose PNP such as 2N3906.

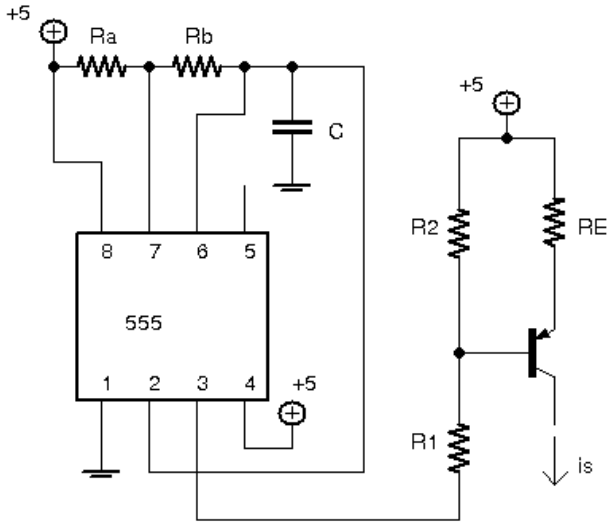

FIG. 6: Pulse train circuit for current source. $R_a = 100k\Omega$ potentiometer, $R_b = 5k\Omega$ potentiometer, $C = 0.1\mu$f, $R_1 = 22k\Omega$, $R_2 = 10k\Omega$, and $R_E = 1k\Omega$ potentiometer.

III. 3-TRANSISTOR MODEL

A simple three-transistor circuit that has excitation pulses similar to the FN system is shown in Figure 7(a). The capacitor voltage V and the transistor-base voltage V_b are the excitable and inhibitory variables analogous to u and v in the FN model. Figure 8 shows V and V_b when $R_s = 100k\Omega$. Also shown is the prediction from the model described below.

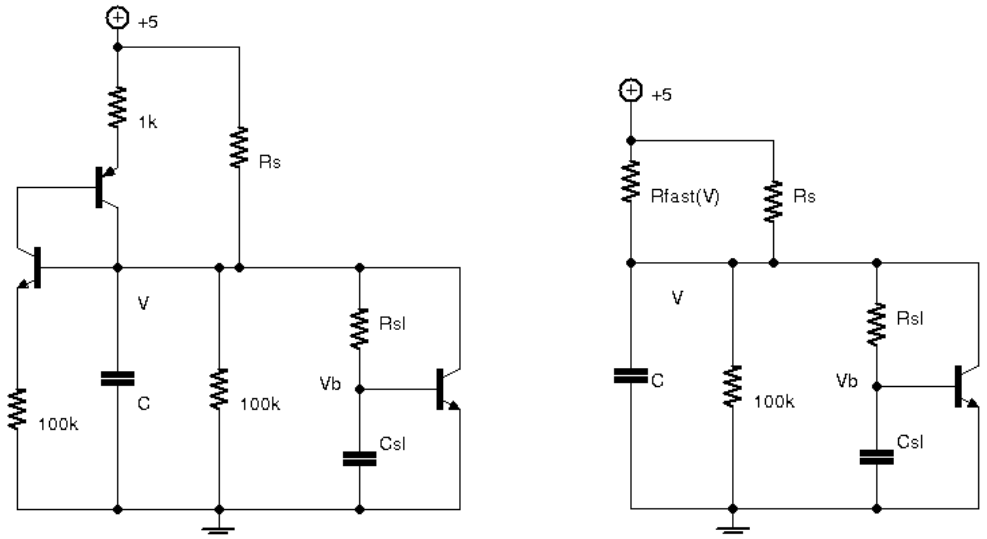

(a)Complete circuit (b)Simple model

FIG. 7: Three-transistor excitable circuit and its simplified model in which the two transistors responsible for the fast-response positive feedback have been replaced by $R_{fast}(V)$. $C = 0.47\mu f$, $C_{sl} = 1\mu f$, and $R_{sl} = 47k\Omega$. R_s controls the period. The npn and pnp transistors are 2N3904 and 2N3906 respectively.

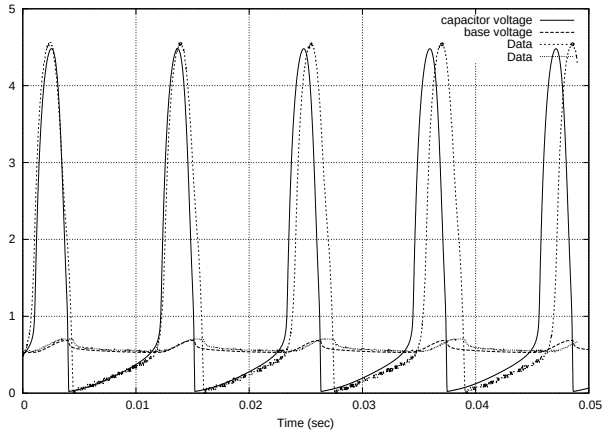

FIG. 8: Numerical calculation and experimental data for excitation pulses from the 3-transistor excitable circuit.

It is possible to use a mathematical model which calculates all voltages and currents of the circuit (SPICE for example). However the goal here is to obtain a two-variable model similar to the FN system. Therefore we model the circuit by the simpler circuit shown in Fig 7(b) in which the two transistors responsible for the fast response positive feedback

have been replaced by resistance $R_{fast}(V)$ which is a function of capacitor voltage V. The remaining transistor provides the slow response negative feedback and is modeled using the Ebers-Moll equations.[8,9] Resistor R_s plays the role of a source term similar to $s(t)$ in the FN system. If R_s is removed, this is analogous to setting $s(t) = 0$ in Eq. 1a. A wide range of pulse periods can be obtained by varying R_s from about $10k\Omega$ to over $1M\Omega$.

The Ebers-Moll model for transistors is often unfamiliar to physics students. The advantage of this model is its applicability to all situations for the transistor, from fully off with base voltage equal to emitter voltage all the way to fully on (saturation) with collector voltage nearly equal to emitter voltage. Thus this transistor model covers both linear amplification and switching applications. A brief explanation of the model follows, however familiarity with the basics of bipolar junction transistors is assumed.

The standard current-voltage relation for a PN semiconductor junction is

$$I(V) = I_s\left(\exp\left(\frac{V}{V_T}\right) - 1\right) \tag{4}$$

where $V_T = kT/e \approx 25mV$ at room temperature and I_s is a reverse saturation current. For an NPN bipolar junction transistor the base-emitter and base-collector form opposing PN junctions. A voltage across one of the junctions causes current as given by Eq. 4. The transport factor α is the fraction of this current that diffuses across the base region thereby flowing through the second junction. The difference between the currents at the two junctions is accounted for by the base current. In addition, the voltage across the second junction causes current given by Eq. 4 and its associated current through the first junction given by a transport factor for that direction of current flow. The result is that the transistor's collector and emitter currents each have two contributions, one similar to Eq. 4 due to the junction voltage at that terminal and the other due to the transport current associated with the voltage at the other junction. Ebers and Moll show that the emitter and collector currents are:[8]

$$I_C = -\frac{I_s}{\alpha_r}\left(\exp\left(\frac{V_{BC}}{V_T}\right) - 1\right) + I_s\left(\exp\left(\frac{V_{BE}}{V_T}\right) - 1\right) \tag{5a}$$

$$I_E = \frac{I_s}{\alpha_f}\left(\exp\left(\frac{V_{BE}}{V_T}\right) - 1\right) - I_s\left(\exp\left(\frac{V_{BC}}{V_T}\right) - 1\right) \tag{5b}$$

Each transport factor is related to the more familiar current gains β_f and β_r by $\beta = \alpha/(1-\alpha)$. A transistor is specified by β_f, β_r, and I_s. SPICE values from the data sheet for a 2N3904 are $\beta_f = 416$, $\beta_r = 0.737$, and $I_s = 6.7 \times 10^{-15}$.

Now we express the collector and base currents for the slow-response transistor in Fig. 7(b) in terms of the capacitor voltage V, base voltage V_b, and the transistor parameters. Noting that $V_{BE} = V_b$, $V_{BC} = V_b - V$, and that $1/V_T = 40$ volts^{-1}, the base current $I_B = I_E - I_C$ is

$$I_B(V, V_b) = \frac{I_s}{\beta_f}\left(e^{40V_b} - 1\right) + \frac{I_s}{\beta_r}\left(e^{40(V_b - V)} - 1\right) \tag{6}$$

and the collector current is

$$I_C(V, V_b) = -\frac{I_s}{\beta_r}\left(e^{40(V_b - V)} - 1\right) + I_s\left(e^{40V_b} - e^{40(V_b - V)}\right) \tag{7}$$

Analysis of the simplified circuit in Fig. 7(b) results in the system of equations for capacitor voltage V and base voltage V_b:

$$C\frac{dV}{dt} = \frac{5 - V}{R_{fast}(V)} + \frac{5 - V}{R_s} - \frac{V}{100k} - \frac{V - V_b}{R_{sl}} - I_C(V, V_b) \tag{8a}$$

$$C_{sl}\frac{dV_b}{dt} = \frac{V - V_b}{R_{sl}} - I_B(V, V_b) \tag{8b}$$

A suitable model for $R_{fast}(V)$ is found by inspection of the fast-response portion of the circuit in Fig 7(a). As V increases from zero and passes through some threshold value V_{th}, the two transistors turn on allowing current to flow through the series combination of the $1k\Omega$ and pnp transistor. This provides the threshold-triggered positive feedback that rapidly charges the capacitor. Thus $R_{fast}(V)$ needs to be a steep transition from very large resistance down to $1k\Omega$. For the purposes of numerical integration it is preferable to use a smooth well defined function (as opposed to a step function). The function we use is

$$R_{fast}(V) = 1000\left(1 + e^{w(V_{th} - V)}\right) \tag{9}$$

Figure 9 shows Eq 9 using parameters $w = 9$ and $V_{th} = 1$ along with the experimentally determined resistance obtained by measuring the current through the $1k\Omega$ (and the pnp transistor) as a function of capacitor voltage V.

Variables V and V_b were computed numerically using Eq 8 with $R_s = 100k\Omega$. The resulting excitation pulses are shown in Fig 8. The phase-space plot in Fig 10 shows the characteristic reverse-N shape for the V-nullcline that results in the excitation pulses. The nullclines were found by setting the derivatives in Eq 8 to zero and numerically finding the zeros of V_b as a function of V.

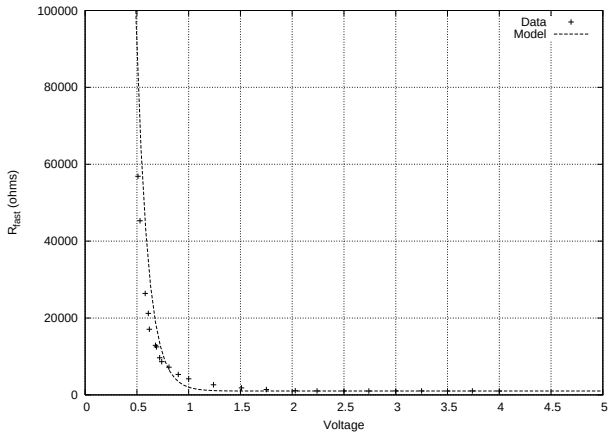

FIG. 9: Measured resistance of the 2-transistor fast-response positive feedback part of the 3-transistor excitable circuit, and its calculated replacement $R_{fast}\,(V)$ from Eq 9.

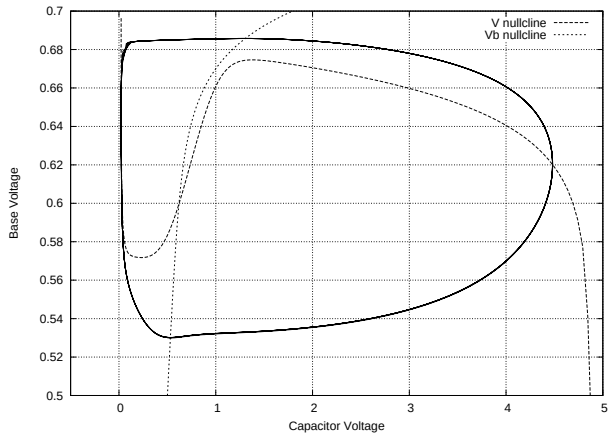

FIG. 10: Numerical calculation of phase space plots of the excitation pulses and nullclines for the 3-transistor circuit.

IV. EXAMPLE INVESTIGATIONS

As an example of the type of system that can be investigated by this method we construct a reaction-diffusion excitable medium by coupling excitable cells together with resistor R_d as shown in Fig 11. This is similar to what Nagumo did with his tunnel diode based FN circuit.[2] This system represents a one-dimensional spatially extended excitable medium similar to a nerve.

Terms must be added to the right side of Eq 8a (or 2a) to account for current flow to and from neighboring cells. These two terms are rearranged into the form of a diffusion term.

$$\frac{V_{i+1}-V_i}{R_d}-\frac{V_i-V_{i-1}}{R_d}=\frac{V_{i+1}-2V_i+V_{i-1}}{R_d}\Rightarrow\frac{\Delta x^2}{R_d}\frac{\partial^2 V}{\partial x^2} \tag{10}$$

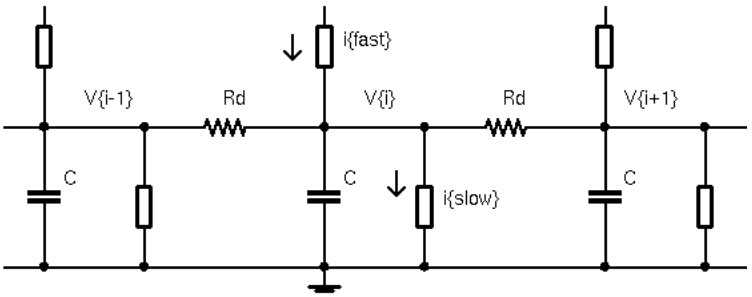

FIG. 11: Reaction-diffusion circuit for propagation of excitation pulses.

Δx is the distance between neighboring cells of the medium. Diffusion is characterized by the diffusion coefficient D where the characteristic time for diffusing the distance Δx is $\Delta x^2/D$. Thus the connection between diffusion and the electrical parameters is

$$\frac{\Delta x^2}{D} = R_d C \tag{11}$$

The characteristic time for diffusion between neighboring cells corresponds to the RC time constant for the capacitance and coupling resistor R_d.

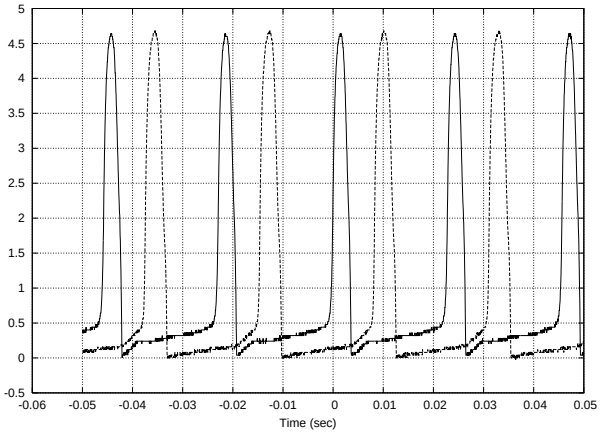

FIG. 12: Voltages measured at self-firing (first) cell and third cell demonstrating propagation of excitation pulse.

Since multiple excitable cells are required we choose the electronically simpler 3-transistor circuit in Fig 7(a). A self-firing cell with $R_s = 330k\Omega$ is the first cell followed by two cells without R_s. The cells are coupled with $R_d = 100k\Omega$. Figure 12 shows the capacitor voltages of the first and third cells. This demonstrates that excitations initiated in the first cell propagate along the linear array of cells. The effect of the diffusion coefficient

on the existence of and speed of propagating pulses may be investigated by changing R_d. Corresponding predictions involve a good computational physics project since they involve numerical solution of partial differential equations.

Another interesting topic is how excitable media respond to pacing. This is relevant to cardiac dynamics including arrhythmias. A simple example that begins to address this topic is to apply a pulse train stimulation to one of the excitable circuits presented here. We use the circuit shown if Fig 6 and the FN circuit. Figure 13 shows the measured capacitor voltage which demonstrates alternating amplitude pulse dynamics known as alternans when referring to cardiac signals.

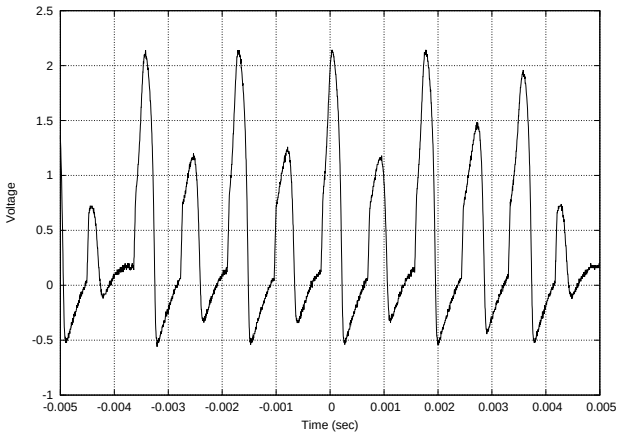

FIG. 13: Measured capacitor voltage for Fitzhugh-Nagumo circuit with pulse train stimulation set fast enough to cause alternans.

Other possible investigations include applying a pulse train to the reaction-diffusion system and investigations of coupled oscillators.

Acknowledgments

This research was supported by an award from the Research Corporation. Matthew J. Lanctot did some preliminary work on this project. We thank Joseph Starobin for useful discussions.

---

* Currently at Dept. of Physics, NYU.

† Electronic address: ehhellen@uncg.edu

[1] R. Fitzhugh, "Impulses and physiological states in theoretical models of nerve membrane," Biophys. J. **1**, 445–466 (1961).

[2] J. Nagumo, S. Arimoto, and S. Yoshizawa, "An active pulse transmission line simulating nerve axon," Proc. IRE **50**, 2061–2070 (1962).

[3] G. Y. Yuan, S. G. Chen, and S. P. Yang, "Eliminating spiral waves and spatiotemporal chaos using feedback signal," Eur. Phys. J. B **58**, 331–336 (2007).

[4] P. H. Bunton, W. P. Henry, and J. P. Wikswo, "A simple integrated circuit model of propagation along an excitable axon," Am. J. Phys. **64**, 602–606 (1996).

[5] R. C. Hilborn, *Chaos and Nonlinear Dynamics* (Oxford University Press Inc., New York, 2003), 2^{nd} ed., 97–99.

[6] J. C. Comte and P. Marquié, "Generation of nonlinear current-voltage characteristics. A general method," Int. J. Bifurcat. Chaos **2**, 447–449 (2002).

[7] P. Marquié, J. C. Comte, and S. Morfu, "Analog simulation of neural information propagation using an electrical Fitzhugh-Nagumo lattice," Chaos Soliton. Fract. **19** 27–30 (2004).

[8] J. J. Ebers and J. L. Moll, "Large signal behavior of junction transistors," Proc. IRE **42**, 1761–1772 (1954).

[9] J. D. Irwin and D. V. Kerns Jr., *Introduction to Electrical Engineering* (Prentice Hall, Upper Saddle River, NJ, 1995) p 333.